

Iron–sulfur–phosphorus cycling in the sediments of a shallow coastal bay: Implications for sediment nutrient release and benthic macroalgal blooms

Tim F. Rozan, Martial Taillefert,¹ Robert E. Trouwborst, Brian T. Glazer, and Shufen Ma

College of Marine Studies, University of Delaware, Lewes, Delaware 19958

Julian Herszage

INQUIMAE and Departamento de Química Inorgánica, Analítica y Química Física, Facultad de Ciencias Exactas y Naturales, Universidad de Buenos Aires, C1428EHA Buenos Aires, Argentina

Lexia M. Valdes, Kent S. Price, and George W. Luther III²

College of Marine Studies, University of Delaware, Lewes, Delaware 19958

Abstract

We conducted a study to determine the seasonal relationship between iron, sulfur, and phosphorus in the upper sediments and pore waters of a shallow intercoastal bay. From April 1999 to September 2000, sediment cores were collected from Rehoboth Bay, Delaware. Analyses of the sediments in the upper 4 cm revealed that redox conditions controlled Fe-S-P concentrations in the sediments, pore waters, and overlying water. Monthly sampling showed a marked decrease in the reactive solid phase P pool (ascorbate leachable fraction, ASC-P) and sharp increases in soluble P (measured as PO_4^{3-}) in pore waters and overlying waters, as the conditions became more reducing throughout the summer months. These changes were paralleled by decreases in the amorphous Fe(III) (ascorbate leachable fraction, ASC-Fe) and total Fe(III)oxyhydroxide pools [dithionite extracted fraction, Fe(III)_{oxide}] and increases in solid FeS/FeS₂. The release of soluble P from sulfidic sediments to oxygenated overlying waters only occurred during periods of solid FeS/FeS₂ production, which indicates that Fe(III) oxides act as a barrier to diffusive P flux. During these anoxic conditions, the regenerative P appears to induce secondary benthic algal blooms and promotes eutrophication in these inland bays through late summer. By the late fall and into early spring, sulfide production diminished and oxic conditions were reestablished as indicated by increases in solid amorphous and crystalline Fe(III) oxides and decreases in FeS/FeS₂ concentrations. During this period, increasing ASC-Fe concentrations correlated with increases in ASC-P concentrations and decreases in pore-water PO_4^{3-} . The seasonal correlations between Fe-S-P indicate that Fe redox chemistry controls sediment P flux to the overlying water column.

Nutrient cycling in estuarine systems is of primary concern due to its direct effect on primary productivity. Excessive nutrient loading in estuaries has led to increased organic matter production, and its subsequent decay has created extensive suboxic or anoxic zones and toxic sulfide levels in many productive estuarine systems (e.g., Officer et al. 1984). In many coastal environments, nitrogen species have traditionally been described as the limiting nutrient (e.g., Mortimer et al. 1999). However, with increased urbanization, fertilizer use, and runoff, many systems such as inland bays and estuarine waters may now be phosphorus limited on a seasonal basis instead.

The removal of phosphate from estuarine waters can increase the dissolved N:P to above the generalized 16:1 Redfield ratio, limiting primary productivity. However, if sufficient PO_4^{3-} is released from the sediments and allowed

to diffuse back into the overlying water, sufficient nutrients are available for additional organic matter production. Such a mechanism may explain the secondary algal growth observed in nitrate rich environments such as coastal bays (Timmons and Price 1996; Cerco and Seitzinger 1997) following the onset of anoxic conditions in shallow sediments.

Although seasonal phosphorus cycling in these intercoastal environments is not well documented, data have been amassed on the mechanisms responsible for P cycling in near shore/continental margin sediments (e.g., Krom and Berner 1981; Klump and Martens 1987; Sundby et al. 1992; Gunnars and Blomqvist 1997; Anschutz et al. 1998; Golterman 2001). In these sediments, phosphorus has been classified into four distinct fractions: organic P, Fe bound P, authigenic P minerals (such as carbonate fluorapatite, CFA) and detrital P minerals (Ruttenberg and Berner 1993). However, only organic P (nonrefractory organics, Ingall and Jahnke 1997) and Fe bound P (Krom and Berner 1981) appear to be involved in P regeneration with subsequent release to pore waters and overlying waters via the decomposition of organic matter (Ingall and Jahnke 1997) and the reduction of solid iron oxides (Krom and Berner 1981). McManus et al. (1997) showed that P release to overlying waters was related to Fe bound P rather than organic matter decomposition. In a detailed study on Fe bound P, Anschutz et al. (1998) showed that PO_4^{3-} is primarily associated with amorphous Fe

¹ Present address: School of Earth and Atmospheric Sciences, Georgia Institute of Technology, Atlanta, Georgia 30332.

² Corresponding author.

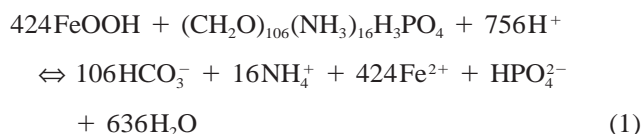
Acknowledgments

This project was funded by the NOAA office of Sea Grants (NA16RG0162-03) to G.W.L. and by the Delaware Center for the Inland Bays to K.S.P. J.H. was partially supported by a grant from the Science Foundation of Argentina. R.E.T. was partially supported by a grant from the Stichting Molengraaff Fonds.

(ascorbate leachable, ASC-Fe) and not crystalline Fe in a variety of sediments. In addition, they found that CFA is not leachable by the methods used to measure Fe bound P.

The extent of P release is thought to be controlled either by the redox conditions at the sediment-water interface (Krom and Berner 1981) and/or by the formation of authigenic P minerals (CFA) in supersaturated pore waters (Ruttenberg and Berner 1993; Slomp et al. 1996). In continental margin sediments, McManus et al. (1997) found negligible P release from sediments where the O₂ penetration depth exceeded 5 mm, whereas Ingall and Jahnke (1997) found sharp decreases in the P flux from sediments when bottom waters were fully oxygenated. In both cases, the removal mechanism appears to be P adsorption on iron oxides in the oxic/suboxic sediments. Alternatively, P removal due to mineral precipitation may occur when pore-water phosphate levels are increased quickly due to iron reduction events (Slomp et al. 1996). However, with only sparse field data existing on seasonal P cycling in sediments (Klump and Martens 1987; Slomp et al. 1998, including no specific data on seasonal controls of redox variations in the solid Fe fractions: amorphous oxides, crystalline oxides, and iron sulfides), our understanding of how phosphorus is annually recycled in shallow water systems is very limited.

In experimental studies on sediment cores, Gunnars and Blomqvist (1997) showed that the reduction of FeOOH in freshwater and brackish sediments was predominately responsible for the release of PO₄³⁻ to the overlying water column. In freshwater sediments, the released Fe:P ratio was found to equal 1. Since FeOOH reduction of organic matter produces a much higher Fe:P ratio (Eq. 1), the released P was



attributed to dissolution of FeOOH-phosphate complexes. In coastal sediments, the release of Fe:P was found to be $\ll 1$ (Gunnars and Blomqvist 1997), which probably resulted from subsequent Fe removal as iron sulfides. In estuarine sediments, Fe(II) has been shown to be quickly and effectively removed from pore waters by precipitation of solid FeS and FeS₂ formation in the presence of H₂S (Taillefert et al. 2000).

Chemical profiles in anoxic sediments have revealed the interaction between iron and sulfur during early diagenesis (e.g., Canfield 1989; Kostka and Luther 1995). In intertidal sediments where sulfide occurs in significant concentrations, the reductive dissolution of Fe(III) oxyhydroxide phases is quickly followed by formation of FeS_{aq} (Eq. 2; Theberge and Luther 1997), FeS_s, and FeS₂. Pyritization in anoxic conditions is fast and occurs by reaction between H₂S or S(0) (as S₈ or polysulfides [S_x²⁻]) and aqueous (or solid) FeS (Rickard 1975; Luther 1991; Rickard 1997; Rickard and Luther 1997) according to Eqs. 3–4:



Because iron sulfide minerals have a low point of zero charge and do not adsorb phosphate at neutral pH (Bebie et al. 1998), these iron-sulfide reactions effectively solubilize solid P and maintain PO₄³⁻ in pore waters, while removing Fe(II) from the solution. Thus, changes in sediment redox conditions and sulfide production probably control PO₄³⁻ cycling in shallow coastal sediments and overlying waters.

The goal of this study was to follow seasonal changes in the solid and pore-water concentrations of Fe-S-P in the upper sediments of a shallow coastal bay. By measuring Fe-S-P fractions, we expected to observe the natural coupling of Fe-S-P in sediments to determine the biogeochemical controls on PO₄³⁻ cycling. Release of PO₄³⁻ to overlying waters during sediment anoxic events in summer will enhance macroalgal and phytoplankton blooms, which are known to occur in this ecosystem (Cercu and Seitzinger 1997). Our field experimental approach to measure amorphous and crystalline Fe(III) (oxy)hydroxide and iron sulfide phases in addition to soluble P and Fe is in contrast to studies (1) that measure only solid phase and dissolved PO₄³⁻ and/or perform manipulation experiments with cores (e.g., Krom and Berner 1981; Sundby et al. 1992; Gunnars and Blomqvist 1997) and (2) that measure Fe-S-P parameters at only one time of the year (Anschutz et al. 1998).

Study location

Three interconnected embayments (Rehoboth, Indian River, and Little Assawoman bays) comprise Delaware's Sussex County Coastal Bays (Fig. 1). They have a 777 km² watershed, and 83 km² of water surface (Price 1998). The only regular source of seawater from the Atlantic Ocean to the estuaries is through the Indian River Inlet. Flooding tides enter the inlet and flow westward and northward into Indian River and Rehoboth Bays (Wong and Lu 1994). Residence times are estimated to be on the order of 90–100 d for Rehoboth and Indian River Bays (Price 1998). The bays suffer from varying degrees of eutrophication, fueled by both point and non-point source nutrient loading (sewage treatment plants, septic systems, and agricultural and residential runoff). Such nutrient overenrichment results in undesirable phytoplankton and macroalgae blooms, both of which lead to localized declines in light penetration and substantial water column dissolved oxygen fluctuations (Price 1998). Sediment cores for the present study were collected from a well-flushed bottom site in the northwest corner of Rehoboth Bay. The site has a mean low water depth of 1 m and salinity of 29‰, and it supports a seasonal benthic macroalgae community.

Methods

Sampling—Sediment cores were collected from April 1999 to September 2000, on a monthly basis from the late spring (April) through the fall (October) and once during the winter. To collect cores, an 80-mm diameter transparent acrylic tube, which was attached to an aluminum pole screwed into an Al bracket, was inserted into the sediments. The metal bracket was clamped around the outside of the

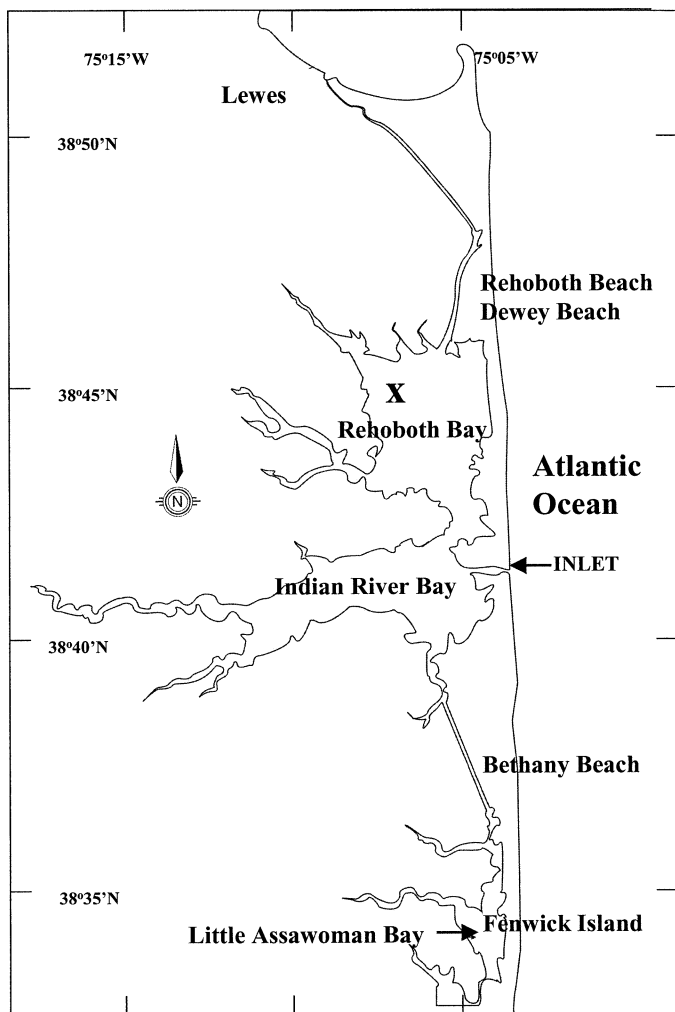


Fig. 1. A map of Rehoboth Bay Delaware showing the sampling location (X). Sediment cores were all collected within a 150 m² area.

acrylic tube and also housed a plastic lid (grooved along its sides), which allowed water to flow along the sides and out of the top of the acrylic tube as the core was pushed into the sediment. On extrusion, the core was sealed with the flat top part of this plastic lid, which allowed for sediment extraction. Thus, intact overlying water samples were retrieved without contamination from the rest of the water column. The cores were then capped, sealed, and transported back to the laboratory for analysis within 1.5 h of collection. In all cores, at least 20 cm of overlying water were retained by the plastic lid, which minimized physical disturbance during transport.

Macroalgae sampling—An aluminum dredge sled was used to sample macroalgae as described in Timmons and Price (1996). The total capacity of the sled is 250 liters. Data are the average of two 2-min tows at a constant boat speed (linear distance is less than 90 m). Data are expressed in units of milliliters of wet biomass per minute.

Microelectrode data—Solid state gold-amalgam (Au/Hg) microelectrodes (Brendel and Luther 1995; Luther et al. 1998) were used to measure pore-water dissolved O₂, S(-2), Fe²⁺, Mn²⁺, FeS_{aq}, and Fe(III). These results are reported in detail in Taillefert et al. (2002) and show that the O₂ penetration depth was typically less than 1 mm.

Pore-water extractions and measurements—The sediment was sliced under a N₂ atmosphere in a glove bag into 3–7-mm thick slices and placed in acid-washed 50-ml centrifuge tubes. The pore waters were then extracted by centrifugation under a N₂ atmosphere, collected in syringes, and filtered with disposable 0.2- μ m filters (Whatman Puradisc 25 AS) into clean 5-ml Falcon tubes for subsequent analysis. Aliquots of the collected pore waters were separated for Fe(II), Fe_T [defined as dissolved Fe_T = dissolved Fe(III) + dissolved Fe(II)], NH₄⁺, and PO₄³⁻ analysis. Dissolved Fe(III) can be determined by the difference between Fe_T and Fe(II).

Dissolved Fe(II) and PO₄³⁻ were analyzed by colorimetry using a Spectronic 601 (Milton Roy) and NH₄⁺ by the flow injection method of Hall and Aller (1992). PO₄³⁻ concentrations were determined using the molybdate-blue complexation method (Koroleff 1983), while Fe(II) was determined by the ferrozine method (Stookey 1970). The molybdate-blue complexation method consisted of adding 0.6 ml of sample to 4.4-ml deionized water and 0.8 ml of ammonium molybdate solution (made as per Koroleff 1983). Ascorbic acid was added to allow for molybdate-blue color formation, and after 2 h absorbance was measured at 885 nm. A blank correction was used to account for ascorbic acid interference. For Fe(II) determinations, samples were immediately stabilized in the ferrozine after filtration under a N₂ atmosphere. The ferrozine solution consisted of 50% of a 2.5 M ammonium acetate buffer and 50% of a 0.01 M ferrozine. Samples were allowed to stand for less than 30 min for color development, followed by absorbance measurement at 562 nm. For Fe_T determination, 0.1 M HCl-hydroxylamine was added to the samples to reduce any dissolved Fe(III) to Fe(II). Fe_T samples were allowed to stand for 24 h at room temperature to ensure complete Fe(III) reduction had taken place. Then the Fe_T samples reacted with ferrozine solution for subsequent Fe analysis.

Solid phase extraction and measurements—For each depth interval, the centrifuged sediment was subsampled to provide three replicates for separate determinations of amorphous iron (ASC-Fe), reactive phosphate (ASC-P), total amorphous and crystalline iron [Fe(III)_{oxide}], FeS, and pyrite. The ASC-Fe and ASC-P were defined as the material leached from ascorbic acid solution (as per Anschutz et al. 1998) and includes some FeS (Kostka and Luther 1994). Crystalline iron (Fe_{crys}) was defined as the reactive Fe leached during a dithionite extraction minus the ASC-Fe fraction (Kostka and Luther 1994). Fe_{crys} has been shown to contain large portions of crystalline and amorphous Fe(III)oxides, and traces of reactive Fe silicates (Canfield 1989; Kostka and Luther 1994).

Amorphous iron (ASC-Fe)/reactive phosphate (ASC-P): Separate ascorbic acid leaches were used for either Fe or

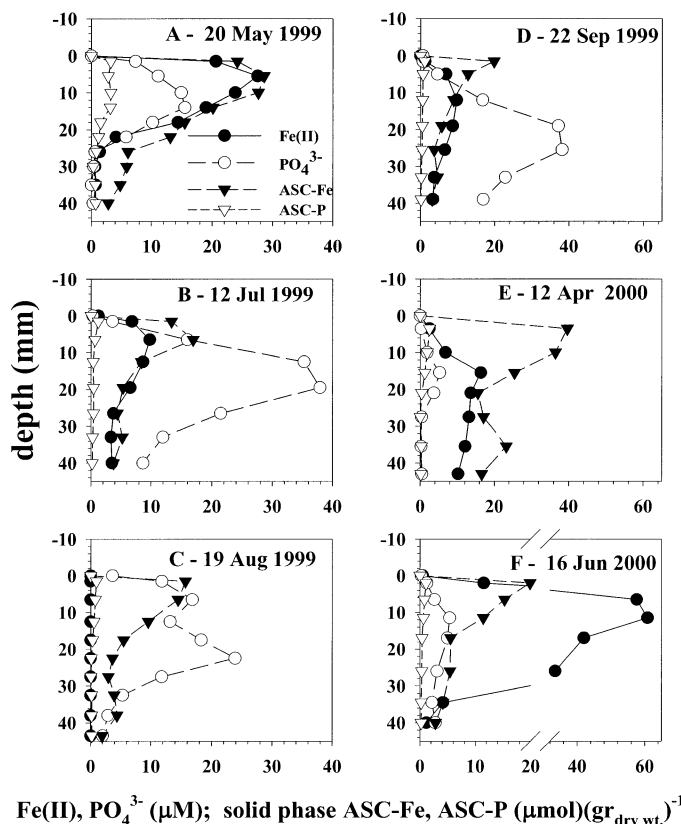


Fig. 2. Sediment profiles from (A) May, (B) July, (C) August, and (D) September 1999 and (E) April and (F) June 2000 cores (Note x -axis break in F). Fe(II) and PO_4^{3-} are given in $\mu\text{mol L}^{-1}$. ASC-Fe and ASC-P are given in $\mu\text{mol}(\text{g}_{\text{dry wt.}})^{-1}$. Negative depth values representing depth of overlying water above the sediment-water interface, while positive values are sediment depths below the interface. Zero depth represents sediment-water interface.

PO_4^{3-} in accordance with the method of Anschutz et al. (1998). Ten milliliters of ascorbic acid solution were added to 0.4 g of sediment. The ascorbic acid solution consisted of 10 g Na-citrate and 10 g bicarbonate in 200 ml of deaerated deionized water to which 4 g of ascorbic acid were slowly added to a pH of 8. The samples were then put in a water bath (50°C) and shaken at 200 rpm. After 24 h, the samples were filtered ($0.2 \mu\text{m}$) and measured for either Fe or PO_4^{3-} (see above) to give ASC-Fe and ASC-P, respectively.

Total Fe(III) $[\text{Fe(III)}]_{\text{oxide}}$ (amorphous + crystalline): Approximately 0.25 g of sediment was mixed with 10 ml of dithionite solution. The dithionite solution was prepared daily by dissolving 20 g of dithionite into a 200-ml mixture of 0.35 M Na-acetate/0.2 M Na-citrate, which had been deaerated by purging with N_2 for 1 h. The samples were then shaken at 200 rpm for 2 d at room temperature. The extract was filtered ($0.2 \mu\text{m}$) and measured for Fe_T by the ferrozine method as above.

Pyrite/acid volatile sulfide: Pyrite (FeS_2) and acid volatile sulfide (AVS) were extracted from dried and wet sediments,

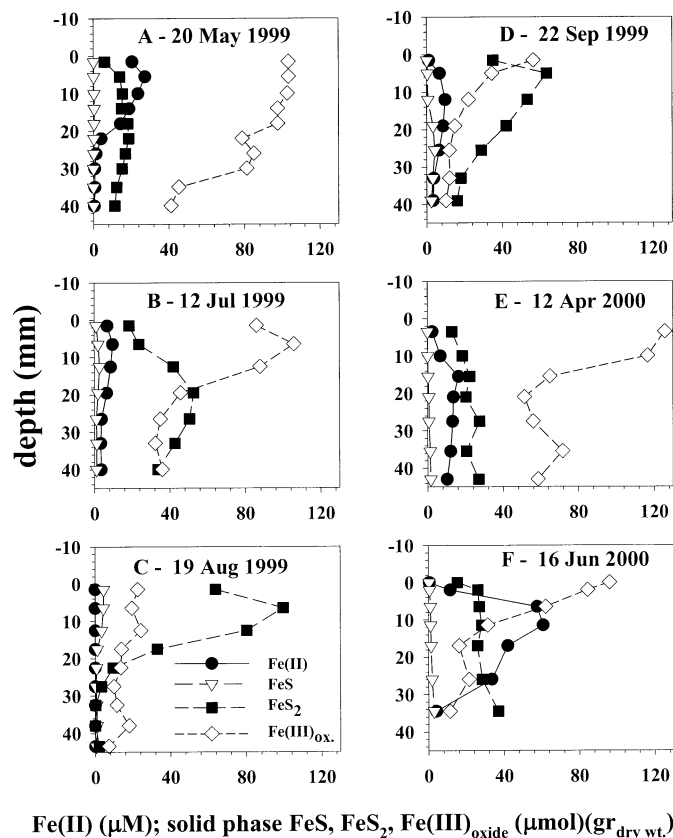


Fig. 3. Sediment profiles from (A) May, (B) July, (C) August, and (D) September 1999 and (E) April and (F) June 2000 cores. Fe(II) is given in $\mu\text{mol L}^{-1}$, whereas FeS (AVS), FeS_2 , and $\text{Fe(III)}_{\text{oxide}}$ (all amorphous and crystalline Fe(III) phases) are given in $\mu\text{mol}(\text{g}_{\text{dry wt.}})^{-1}$. Zero depth represents sediment-water interface.

respectively. FeS_2 determination was accomplished by reduction with acidified Cr(II) and AVS determination by acidification with 3 M HCl according to the methods described in Luther et al. (1992). To remove FeS, the sediment was dried for 24 h at 80°C . To remove S(0) and organic S, the dry sediments were leached with acetone for 24 h prior to acidified Cr(II) addition. A Jones reduction column was used daily to reduce 1 M CrCl_3 (in 1 M HCl) to Cr(II). The bisulfide produced by these two extraction schemes was purged with N_2 and trapped in 1 M NaOH prior to measurement by cathodic square wave voltammetry with a hanging mercury drop electrode system (model 303A, EG&G Princeton Applied Research coupled to a DLK-100A electrochemical analyzer from Analytical Instrument Systems).

Results

A total of 13 cores were collected from northwest Rehoboth Bay covering the period from April 1999 to September 2000. ASC-P (80–90%) typically was found concentrated primarily in the upper 2–4 cm of the sediments. For this reason, this paper focuses only on the Fe-S-P fractions in the upper sediments. In Figs. 2 and 3, we present representative data from six cores to show seasonal changes. Figure

Table 1. Covariance–variance matrix for the soluble and solid Fe-S-P data measured in the upper 4 cm of the sediments of Rehoboth Bay, Delaware. Correlation coefficients were calculated from data collected from the upper 4 cm (eight depth intervals) in the 13 cores collected from April 1999 to September 2000. Bold values in Table 1 represent correlations with significant probabilities <0.05.

Variable	ASC-Fe	Fe _{crystalline}	ASC-P	FeS	FeS ₂	Fe(II)	Fe(III)	PO ₄ ³⁻
ASC-Fe	1.0	0.76	0.74	0.052	0.24	-0.19	-0.047	- 0.41
Fe _{crystalline}		1.0	0.71	0.056	0.21	-0.14	-0.11	- 0.32
ASC-P			1.0	-0.12	0.16	-0.20	0.11	-0.23
FeS				1.0	0.69	-0.29	0.0923	- 0.32
FeS ₂					1.0	-0.067	0.12	- 0.32
Fe(II)						1.0	0.076	0.046
Fe(III)							1.0	-0.093
PO ₄ ³⁻								1.0

2A–F gives dissolved Fe²⁺ and PO₄³⁻ and solid phase ASC-Fe and ASC-P, whereas Fig. 3A–F gives solid phase FeS, FeS₂, and Fe(III)_{oxide}. Table 1 summarizes correlations from all samples in every core.

The profiles of ascorbate-reactive PO₄³⁻ (ASC-P), ascorbate-reactive Fe (amorphous Fe, ASC-Fe), and dithionite-reactive Fe [Fe(III)_{oxide}] in the upper sediments followed similar patterns throughout the year; i.e., there was an enrichment of these chemical species in the surface sediments and a decrease with depth (Figs. 2A–F, 3A–F). ASC-P and ASC-Fe concentrations were highest at the beginning of May 1999, reaching 3.5 and 29 μmol (g_{dry wt})⁻¹, respectively (Fig. 2A). However, as reducing conditions became pronounced through the summer, the concentrations of these fractions decreased markedly to less than 0.7 (ASC-P) and 20 (ASC-Fe) μmol (g_{dry wt})⁻¹ in the bay sediments (Fig. 2B–D). The concentrations of ASC-P and ASC-Fe stayed at these low levels until oxic conditions were reestablished in the winter of 1999 and spring of 2000 (Fig. 2E). Fe(III)_{oxide} concentrations followed the same trends as ASC-P and ASC-Fe (Fig. 3A–E) both within a core and with season (high values in the spring 1999, lower in summer 1999, and higher again in winter and spring of 2000). Fe(III)_{oxide} was comprised mainly of Fe_{cryst} except in the summer (e.g., compare Figs. 2C and 3C) when it was mainly ASC-Fe.

Table 1 shows that pore-water PO₄³⁻ and soluble Fe(II) did not correlate. The concentrations of PO₄³⁻ and soluble Fe are similar to those observed in freshwater sediments (Gunnars and Blomqvist 1997), brackish coastal sediments (Gunnars and Blomqvist 1997), and continental margin sediments (Anschutz et al. 1998). However, only in the coastal and continental margin sediments was a similar dramatic decrease in soluble iron observed, which resulted from the formation of solid FeS and FeS₂.

The FeS and FeS₂ concentrations (Fig. 3A–F) found in Rehoboth Bay fluctuated in accordance with seasonal sulfide production (Taillefert et al. 2002). FeS increased during the summer and ranged from <0.7 μmol (g_{dry wt})⁻¹ to 5 μmol (g_{dry wt})⁻¹. In contrast, pyrite sulfur concentrations were found to be higher by an order of magnitude, ranging from 20 μmol (g_{dry wt})⁻¹ in the spring to a maximum of 100 μmol (g_{dry wt})⁻¹ during summertime anoxic conditions. These values are lower than the average content of the Great Marsh of Delaware (e.g., Kostka and Luther 1995) but similar to other coastal and margin sediments (Canfield 1989; An-

schutz et al. 1998). The summertime increase in FeS (and FeS₂) coincided with the sharp decreases in ASC-Fe and Fe(III)_{oxide}. In May 1999, the FeS fraction was generally negligible compared with the ASC-Fe fraction (Figs. 2A and 3A). However, by July, following the onset of anoxic conditions, FeS formation in the 0–4-cm depth interval increased significantly (Fig. 3A–C). This corresponded with sharp decreases in both the ASC-Fe fraction and soluble Fe(II).

In both years, dissolved H₂S was low (a few micromolar) or not detected in the upper 2 cm of the sediment except in August 1999 (Taillefert et al. 2002), so the onset of anoxic conditions is best defined by solid phase FeS and FeS₂ data. In both years, the transition in the sediment from predominately Fe(III)(oxy)hydroxides to predominately iron sulfides continued throughout the summer and early fall. The reoxidation of iron sulfides to Fe(III)(oxy)hydroxide amorphous and crystalline phases occurred in the winter and spring (Fig. 2D–F and 3D–F) and is similar to the seasonal changes found in salt marsh sediments by Kostka and Luther (1995) and Luther et al. (1992).

The August 1999 microelectrode profile (Fig. 4) showed the extent of pore-water anoxia in the sediments. The entire profile was anoxic with no O₂ penetration. H₂S and FeS_{aq} (Theberge and Luther 1997) were observed throughout the pore-water profile, with no soluble Fe(II) measured by either in situ voltammetric microelectrodes or traditional pore-water analysis. Correspondingly, PO₄³⁻ concentrations were at high levels in the pore water (Fig. 2B–D) and overlying bottom water (Fig. 5A), where micromolar PO₄³⁻ concentrations were detected.

Discussion

Fe-S-P correlation—A covariance–variance matrix was created to help understand the interactions between Fe-S-P in the upper sediments. Using the statistical program JMP IN (SAS Scientific Institute), the Pearson product-moment correlation coefficients were calculated to show the strength of the linear relationships between each pair of measured data. The data used for this calculation included concentrations of dissolved Fe and PO₄³⁻, and of solid Fe and P (FeS, FeS₂, ASC-Fe, Fe_{cryst}, and ASC-P) measured at each depth interval from all 13 cores (Table 1). Pairwise correlations

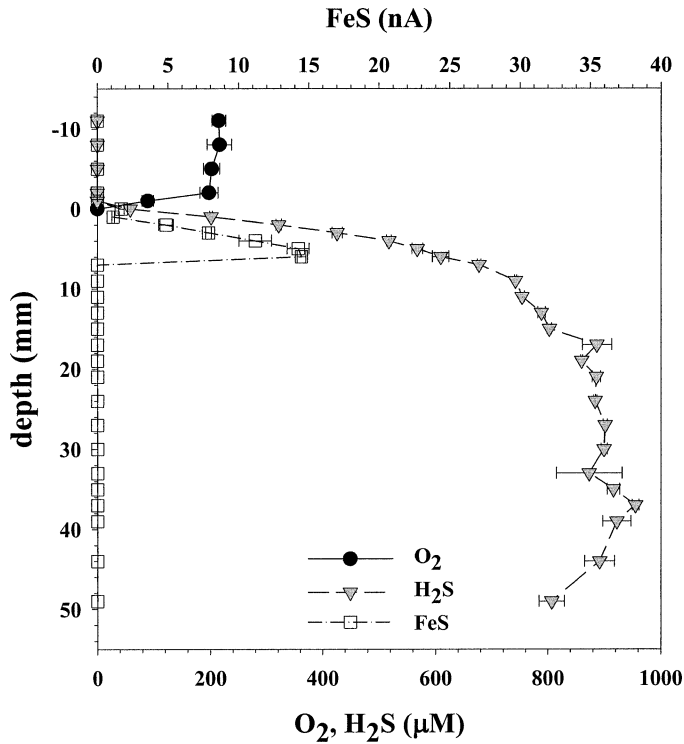


Fig. 4. Microelectrode profile from the August 1999 sediment core. H_2S and O_2 are given in $\mu\text{mol L}^{-1}$. FeS_{aq} values are given in current (nA) due to the inability to quantify (and standardize) the exact forms of the aqueous iron sulfides (Theberge and Luther 1997). No O_2 penetration into the sediments was observed.

were also calculated to show significant probabilities between the different parameters.

The results from the covariance–variance matrix provide insights to the cycling of Fe-S-P in these coastal sediments. The strongest correlations are between ASC-Fe, Fe_{cryst} , and solid ASC-P. The strong relationship between ASC-Fe and solid ASC-P is similar to the results obtained in other studies (e.g., Gunnars and Blomqvist 1997; Anschutz et al. 1998) and provides additional evidence that PO_4^{3-} cycling is being controlled by dissolution of Fe(III) phases and precipitation of FeS and FeS_2 . The correlation between Fe_{cryst} and ASC-Fe probably represents shifts between the amorphous and crystalline fractions. Both production and consumption occur since sulfide reduces these Fe(III) phases with varying reaction rates (Pyzik and Sommer 1981; Canfield 1989; Kostka and Luther 1995; Taillefert et al. 2000) and then precipitates the dissolved Fe(II) as iron sulfide minerals. Also, reoxidation of iron sulfides goes through amorphous to crystalline Fe(III) phases on ageing (e.g., Taillefert et al. 2000).

The hypothesis that Fe/S cycling is controlling PO_4^{3-} cycling in the sediments is further supported by the inverse correlations between PO_4^{3-} and ASC-Fe and between PO_4^{3-} and FeS/FeS_2 . The inverse relationship between PO_4^{3-} and ASC-Fe has a low correlation constant ($r = -0.40$), but it is statistically significant at a P value < 0.005 . The inverse correlations of PO_4^{3-} with FeS and FeS_2 are also significant; however, the lower correlation constants reflect PO_4^{3-} fluxing

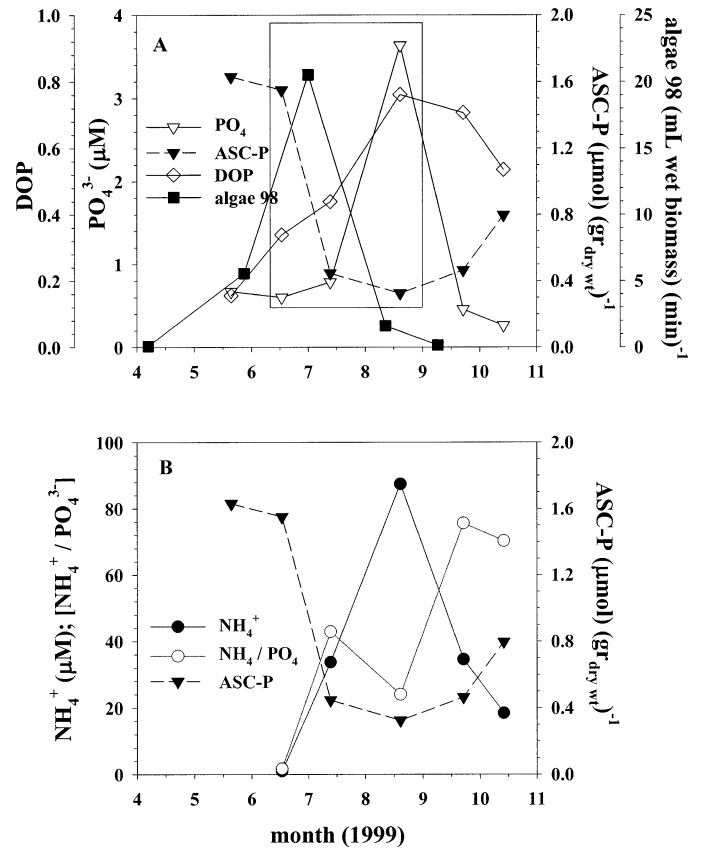


Fig. 5. Surface sediment and overlying water data from the cores in 1999. (A) Surface sediment DOP, solid ASC-P, dissolved PO_4^{3-} and algal data (1998). (B) NH_4^+ and the dissolved $(\text{NH}_4^+):(\text{PO}_4^{3-})$ ratio are given to show that anoxic conditions in the sediments are significant in the summer—especially August, when H_2S is easily detected in pore waters (see Fig. 4).

from the sediment during summer anoxic conditions as observed in Figs. 2 and 5A. In contrast to the solid phase, soluble Fe(II) and PO_4^{3-} in the pore waters did not correlate (e.g., Fig. 2C), which is expected as Fe(II) is removed during iron sulfide formation.

There was a statistically significant inverse correlation between Fe(II) and FeS. These results show that the increased Fe(II), from ASC-Fe dissolution, quickly reacts with sulfides to form FeS. This reaction also explains the weak inverse correlation observed between the ASC-Fe:ASC-P ratio and Fe(II). However, if only the predominately oxic cores (April 1999, May 1999, April 2000) are analyzed, a statistically significant correlation can be found between dissolved Fe(II) and PO_4^{3-} ($r = 0.44$, $p < 0.001$) and a statistically significant inverse correlation can be seen for Fe(II) and ASC-Fe ($r = -0.58$, $p < 0.001$).

Degree of pyritization (DOP)—Increases in solid FeS and FeS_2 during the summer months indicate that sulfate reduction is highly significant in the summer and late fall. This is confirmed by the degree of pyritization (DOP) and the degree of sulphidization (DOS) calculated with Eq. 5 and Eq. 6, which are indicators of use of iron(oxy)hydroxide and

sulfide for pyritization (DOP) and the extent of total iron sulfide precipitation (DOS).

$$\text{DOP} = \frac{[\text{FeS}_2]}{[\text{FeS}_2] + [\text{AVS} - \text{Fe}] + [\text{Dithionite} - \text{Fe}]} \quad (5)$$

$$\text{DOS} = \frac{[\text{FeS}_2] + [\text{FeS}]}{[\text{FeS}_2] + [\text{AVS} - \text{Fe}] + [\text{Dithionite} - \text{Fe}]} \quad (6)$$

The DOP in May 1999 averaged <0.2 in the upper sediments, with only trace amounts of FeS. As the sediments became more reducing in July 1999, the DOP increased to an average value of 0.58, with DOS slightly larger at 0.60. Finally in August, when H₂S was observed throughout the pore-water profile, the DOP reached a maximum value >0.75. Interestingly, the DOS was still only slightly larger than the DOP, which reflected the reaction of FeS and H₂S to form pyrite (Eq. 3). All of these DOP and DOS values are similar to those found in normal marine sediments (Canfield 1989; Kostka and Luther 1995) and show that sulfate reduction, and subsequent FeS and FeS₂ formation, is seasonal in nearshore environments. The change of solid Fe/S phases with season is similar to that found by Kostka and Luther (1995) in salt marsh sediments.

In all cores, the FeS, as measured by acid volatile sulfide (AVS), was found in low concentrations (AVS < 5 μmol [g_{dry wt}]⁻¹). AVS is composed of both aqueous FeS (FeS_{aq}) and solid FeS. FeS_{aq} is a soluble intermediate in pyrite formation that can be detected by voltammetry (Theberge and Luther 1997). In situ voltammetric microelectrode measurements showed only low currents for FeS_{aq} in sediment pore waters (Fig. 4; Taillefert et al. 2002). This suggests that FeS_{aq} is reacting fast with sulfide to form FeS₂ (Eqs. 3 and 4) and not accumulating in sufficient concentration to induce precipitation and solid FeS formation. In the spring, the pH of pore waters was generally above 7. However, in the summer months, due to organic matter mineralization, the pH decreased to less than 6.5, which is below the first pK_a of H₂S (Rickard et al. 1995). This results in H₂S (not HS⁻) being the main sulfide species following sulfate reduction. Rickard (1997) showed that H₂S reacts faster than HS⁻ with FeS_{aq} to form pyrite (Eq. 3). Thus, at the pH found in the sediment, environmental conditions are best to maximize pyritization rates via Eq. 3. This is evidenced by the high concentrations of pyrite found in these sediments, as compared to solid FeS (and the similarity of DOP and DOS values at a given time and depth). Thus, the production of H₂S during the summer months is not only promoting the dissolution of solid Fe(III) (oxy)hydroxide solid phases, but also the removal of soluble Fe(II). Both of these processes enhance PO₄³⁻ cycling in the sediments and overlying water.

Fe:P and N:P relationships—The molar ratio of dissolved Fe(II):P in the pore waters ranged from 4.2 in the spring to less than 0.1 in the summer. This change is also illustrated by the low correlation between Fe(II) and PO₄³⁻ in Table 1. The summer ratios were similar to the results found by Gunnars and Blomqvist (1997) during their experiments on P release from near shore sediments under anoxic conditions. The lower Fe:P ratio is a result of sharp decreases in Fe(II) concentrations during periods of anoxia when

large concentrations of sulfides are produced. The sulfides quickly react with the soluble Fe(II), resulting in the formation and burial of FeS and particularly pyrite (e.g., Fig. 3C).

As shown above, solid ASC-Fe was strongly correlated with ASC-P. The ASC-Fe:ASC-P ratio in the upper sediments under oxic conditions (April 1999) was found to average 8.6. At the height of sediment anoxia (August 1999), the ratio increased to 24.5, which indicated either a disproportionate release of P and/or an addition to the ASC-Fe fraction from Fe_{crys}. Comparison of Figs. 2C and 3C (August 1999) shows that ASC-Fe is most of the Fe(III)_{oxide} fraction as all Fe(III) solid phases are being converted to FeS₂. Based on these data and on the weak correlation between ASC-P and Fe(II), it appears that the Fe_{crys} is converted to ASC-Fe, which in turn is converted to iron sulfide minerals. This type of Fe(III) to Fe(II) transition has been documented in a recent laboratory study that used aged Fe(III) materials (Taillefert et al. 2000). Since little P is contained in the Fe_{crys} fraction (Anschutz et al. 1998), a resulting disproportionate increase in the ASC-Fe fraction will occur that results in a higher Fe:P ratio in the solid fraction with release of dissolved PO₄³⁻ during anoxic periods.

P and macroalgal relationships—Our data show that a significant amount of phosphate is sequestered in amorphous iron phases. However, from June 1999 to July 1999, average ASC-P (Fig. 5A) decreased in the upper 4 cm of sediment from 1.55 to 0.45 μmol (g_{dry wt})⁻¹. Multiplying this difference of 1.10 μmol (g_{dry wt})⁻¹ by the density of the sediment (2.0 g ml⁻¹) and the volume conversion factor (1,000 ml L⁻¹) and then dividing by the sediment volume (2.00 × 10⁻⁴ m³) for our core (4 cm by 8 cm) gives a maximum loss of phosphate from the sediment to the overlying water of 11.0 M m⁻³. This loss of phosphate did not result in an increase of dissolved phosphate in the overlying water for July (see rectangle in Fig. 5A). Instead, this loss of P appears to fuel a benthic algal bloom (N/P ratios in the overlying water also support P uptake, Fig. 5B; see below). Timmons and Price (1996) have shown that maximum baywide macroalgal production in Rehoboth Bay occurs from late June into early July (data for 1998 are plotted in Fig. 5A) and corresponds to an increase in DOP and a decrease in ASC-P (Fig. 5A). Unfortunately, we have an incomplete macroalgal dataset for 1999, but macroalgal content is six times higher in mid-July as compared to mid-August of 1999—consistent with the data in 1998. The average ASC-P in the sediment for August was 0.33 μmol (g_{dry wt})⁻¹ and was similar to that in July and September (Fig. 5). In October, ASC-P increased as temperature and dissolved phosphate decreased, which indicates that, as oxic and suboxic conditions were reestablished in the sediments, phosphate readsorbed to the solid ASC-Fe. The increase in ASC-P also inversely correlates with DOP, which indicates that as FeS₂ oxidizes to ASC-Fe, P binds to Fe in the ASC-Fe fraction. This reaction sequence demonstrates the seasonal cycling of P within this ecosystem, which has a water residence time of about 100 d (Price 1998).

Sulfate reduction produces both phosphate and NH₄⁺ from

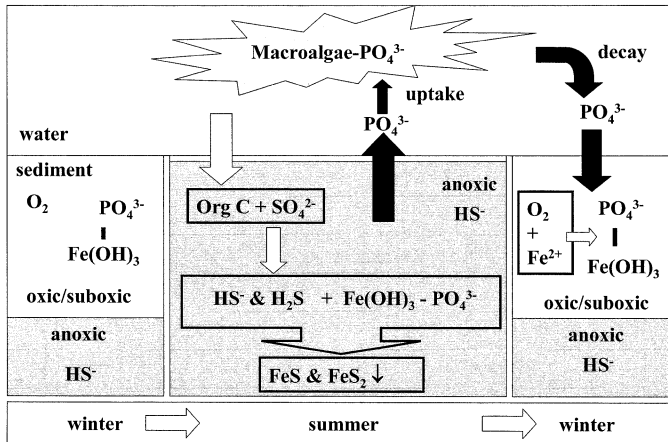
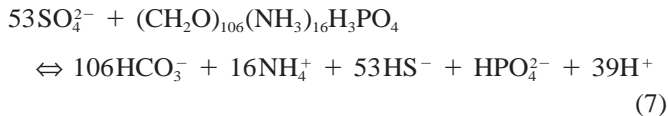


Fig. 6. Schematic of phosphate cycling (indicated with the filled darker arrows) as redox state changes in sediments. Phosphate adsorbed to Fe(III) solid phases is stored in oxic and suboxic sediments in the winter and early spring (lower left), then is converted to the dissolved phase and taken up by macroalgae (with a N:P of 20) in the summer as sulfate reduction occurs in the sediments (center and top) and finally is re-adsorbed to and stored on Fe(III) phases as oxic conditions are reestablished in the sediments in late fall and winter (lower right).

organic matter decomposition (Eq. 7). Under sulfidic conditions in the summer, both nutrients are



produced in the pore water and overlying water (Fig. 5B), but NH_4^+ is released in far greater concentrations, which indicates that phosphate is being utilized. In August 1999, the $\text{NH}_4^+:\text{PO}_4^{3-}$ ratio in the overlying water is 24 and similar to the N:P ratio of 20 reported for macroalgae by Duarte (1991). However, the N:P of 43 is much higher in July, which indicates that the regenerated P was incorporated into secondary benthic macroalgal growth in July and then released by subsequent organic matter decomposition by sulfate reduction. These data, along with higher $\text{NH}_4^+:\text{PO}_4^{3-}$ ratios (58 to 76) in September and October, indicate that phosphate is a limiting nutrient in the bottom water for most of the year. Thus, the release of phosphate from anoxic and sulfidic sediments enhances primary productivity of benthic macroalgae over the short time period in late June to early July.

Sediment cores were collected over a 1-yr period to understand seasonal relationships between Fe-S-P in the upper sediments of a shallow coastal bay. A combination of pore-water and sediment analyses was successfully used to determine transformations between solid and aqueous fractions. The results showed the importance of redox conditions and sulfide production in determining P cycling in sediments from shallow inland bays.

Figure 6 is a schematic diagram that shows shifts in Fe-S-P solution and solid phase fractionation as the sediments became more reducing during the summer and oxidizing in

the late fall and winter. At the beginning of the spring to early summer, soluble Fe, ASC-P, ASC-Fe, and Fe_{cryst} were observed at their highest concentrations, whereas PO_4^{3-} was found at lower concentrations. However, as the summer progressed and the sediments became more reducing, solid Fe(III) oxide phases decreased as iron sulfide mineral phases increased in concentration tenfold with correspondingly high DOP and DOS values. By July, dissolved pore-water phosphate increased threefold, but most of the Fe-bound PO_4^{3-} (ASC-P) was released from ASC-Fe and then lost from the sediment to the overlying water resulting in a bloom of benthic algae. This flux of P to the water column from June to July appears to have enhanced benthic primary productivity in the summer. Because ASC-P and ASC-Fe do not increase until late fall, this regenerated P remains in the water column and stimulates diatom growth, which is significant in this ecosystem until midfall.

References

- ANSCHUTZ, P., S. ZHONG, AND B. SUNDBY. 1998. Burial efficiency of phosphorus and the geochemistry of iron in continental margin sediments. *Limnol. Oceanogr.* **43**: 53–64.
- BEBIE, J., M. A. A. SCHOONEN, M. FUHRMANN, AND D. R. STRONGIN. 1998. Surface charge development on transition metal sulfides: An electrokinetic study. *Geochim. Cosmochim. Acta* **62**: 633–642.
- BRENDEL, P. J., AND G. W. LUTHER III. 1995. Development of a gold amalgam voltammetric microelectrode for the determination of dissolved Fe, Mn, O_2 , and S(-II) in porewaters of marine and freshwater sediments. *Environ. Sci. Technol.* **29**: 751–761.
- CANFIELD, D. E. 1989. Reactive iron in marine sediments. *Geochim. Cosmochim. Acta* **53**: 619–632.
- CERCO, C. F., AND S. P. SEITZINGER. 1997. Measured and modeled effects of benthic algae on eutrophication in Indian River-Rehoboth Bay, Delaware. *Estuaries* **20**: 231–248.
- DUARTE, C. M. 1991. Nutrient concentration of aquatic plants: Patterns across species. *Limnol. Oceanogr.* **37**: 882–889.
- GOLTERMAN, H. L. 2001. Phosphate release from anoxic sediments or 'What did Mortimer really write?' *Hydrobiologia* **450**: 99–106.
- GUNNARS, A., AND S. BLOMQUIST. 1997. Phosphate exchange across the sediment–water interface when shifting from anoxic to oxic conditions: An experimental comparison of freshwater and brackish-marine systems. *Biogeochemistry* **37**: 203–226.
- HALL, P. O. J., AND R. C. ALLER. 1992. Rapid, small-volume, flow injection analysis for ΣCO_2 and NH_4^+ in marine and freshwater. *Limnol. Oceanogr.* **37**: 1113–1119.
- INGALL, E., AND R. JAHNKE. 1997. Influence of water column anoxia on the elemental fractionation of carbon and phosphorus during sediment diagenesis. *Mar. Geol.* **139**: 219–229.
- KLUMP, J. V., AND C. S. MARTENS. 1987. Biogeochemical cycling in an organic-rich coastal marine basin. 5. Sedimentary nitrogen and phosphorus budgets based upon kinetic models, mass balances, and the stoichiometry of nutrient regeneration. *Geochim. Cosmochim. Acta* **51**: 1161–1173.
- KOROLEFF, F. 1983. Determination of phosphorus, p. 125–139. *In* K. Grasshoff, M. Ehrhardt, and K. Kremling [eds.], *Methods of seawater analysis*, 2nd ed. Chemie.
- KOSTKA, J. E., AND G. W. LUTHER III. 1994. Partitioning and speciation of solid phase iron in saltmarsh sediments. *Geochim. Cosmochim. Acta* **58**: 1701–1710.

- , AND ———. 1995. Seasonal cycling of reactive Fe in salt-marsh sediments. *Biogeochemistry* **29**: 159–181.
- KROM, M. D., AND R. A. BERNER. 1981. The diagenesis of phosphorus in a near shore marine sediment. *Geochim. Cosmochim. Acta* **45**: 207–216.
- LUTHER, G. W., III. 1991. Pyrite synthesis via polysulfide compounds. *Geochim. Cosmochim. Acta* **55**: 2839–2849.
- , P. J. BRENDEL, B. L. LEWIS, B. SUNDBY, L. LEFRANÇOIS, N. SILVERBERG, AND D. B. NUZZIO. 1998. Simultaneous measurement of O₂, Mn, Fe, I⁻, and S(-II) in marine pore waters with a solid-state voltammetric microelectrode. *Limnol. Oceanogr.* **43**: 325–333.
- , J. E. KOSTKA, T. M. CHURCH, B. SULZBERGER, AND W. STUMM. 1992. Seasonal iron cycling in the salt-marsh sedimentary environment: The importance of ligand complexes with Fe(II) and Fe(III) in the dissolution of Fe(III) minerals and pyrite, respectively. *Mar. Chem.* **40**: 81–103.
- MCMANUS, J., W. M. BERELSON, K. H. COALE, K. S. JOHNSON, AND T. E. KILGORE. 1997. Phosphorus regeneration in continental margin sediments. *Geochim. Cosmochim. Acta* **61**: 2891–2902.
- MORTIMER, R. J. G., J. T. DAVEY, M. D. KROM, P. G. WATSON, P. E. FRICKERS, AND R. J. CLIFTON. 1999. The effect of macrofauna on porewater profiles and nutrient fluxes in the intertidal zone of the Humber Estuary. *Estuar. Coast. Shelf Sci.* **48**: 683–699.
- OFFICER, C. B., R. B. BIGGS, J. L. TAFT, L. E. CRONIN, M. A. TYLER, AND W. R. BOYNTON. 1984. Chesapeake Bay anoxia: Origin, development and significance. *Science* **223**: 22–27.
- PRICE, K. S. 1998. A framework for a Delaware Inland Bays environmental classification. *Environ. Monit. Assess.* **51**: 285–298.
- PYZIK, A. J., AND S. E. SOMMER. 1981. Sedimentary iron monosulfides: Kinetics and mechanism of formation. *Geochim. Cosmochim. Acta* **45**: 687–698.
- RICKARD, D. T. 1975. Kinetics and mechanisms of pyrite formation at low temperatures. *Am. J. Sci.* **275**: 636–652.
- . 1997. Kinetics of pyrite formation by the H₂S oxidation of iron (II) monosulfide in aqueous solutions between 25 and 125°C: The rate equation. *Geochim. Cosmochim. Acta* **61**: 115–134.
- , AND G. W. LUTHER, III. 1997. Kinetics of pyrite formation by the H₂S oxidation of iron (II) monosulfide in aqueous solutions between 25 and 125°C: The mechanism. *Geochim. Cosmochim. Acta* **61**: 135–147.
- , M. A. A. SCHOONEN, AND G. W. LUTHER, III. 1995. The chemistry of iron sulfides in sedimentary environments, p. 168–193. *In* V. Vairavamurthy and M. A. A. Schoonen [eds.], *Geochemical transformations of sedimentary sulfur*, v. 612, ch. 9. American Chemical Society Symposium Series.
- RUTTENBERG, K., AND R. A. BERNER. 1993. Authigenic apatite formation and burial in sediments from non-up-welling continental margin environments. *Geochim. Cosmochim. Acta* **57**: 991–1007.
- SLOMP, C. P., E. H. EPPING, W. HELDEN, AND W. V. RAAPHORST. 1996. A key role for iron-bound phosphorus in authigenic apatite formation in North Atlantic continental platform sediments. *J. Mar. Res.* **54**: 1179–1205.
- , J. F. P. MALSCHAERT, AND W. V. RAAPHORST. 1998. The role of adsorption in sediment-water exchange of phosphate in North Sea continental margin sediments. *Limnol. Oceanogr.* **43**: 832–846.
- STOOKEY, L. L. 1970. Ferrozine: A new spectrophotometric reagent for iron. *Anal. Chem.* **42**: 779–781.
- SUNDBY, B., C. GOBEL, N. SILVERBURG, AND A. MUCCI. 1992. The phosphorus cycle in coastal marine sediments. *Limnol. Oceanogr.* **37**: 1129–1145.
- TAILLEFERT, M., A. B. BONO, AND G. W. LUTHER, III. 2000. Reactivity of freshly formed Fe(III) in synthetic solutions and (pore)waters: Voltammetric evidence of an aging process. *Environ. Sci. Technol.* **34**: 2169–2177.
- , T. F. ROZAN, B. T. GLAZER, J. HERSZAGE, R. E. TROUBORST, AND G. W. LUTHER, III. 2002. Seasonal variations of soluble organic-Fe(III) in sediment porewaters as revealed by voltammetric microelectrodes, p. 247–264. *In* M. Taillefert and T. F. Rozan [eds.], *Environmental electrochemistry: Analyses of trace element biogeochemistry*, v. 811, ch. 13. American Chemical Society Symposium Series, American Chemical Society.
- THEBERGE, S. M., AND G. W. LUTHER, III. 1997. Determination of the electrochemical properties of a soluble aqueous FeS species present in sulfidic solutions. *Aquat. Geochem.* **3**: 191–211.
- TIMMONS, M., AND K. S. PRICE. 1996. The macroalgae and associated fauna of Rehoboth and Indian River Bays in Delaware. *Bot. Mar.* **39**: 231–238.
- WONG, K.-C., AND X. LU. 1994. Low frequency variability in Delaware's inland bays. *J. Geophys. Res.* **99(C6)**: 683–695.

Received: 4 February 2001

Accepted: 22 April 2002

Amended: 9 May 2002